J Mater Sci (2006) 41:7308–7318
DOI 10.1007/s10853-006-0929-3

Study of infrared spectroscopy and elastic properties of fine and coarse grained nickel–cadmium ferrites

K. B. Modi · M. K. Rangolia · M. C. Chhantbar ·
H. H. Joshi

Received: 1 June 2005 / Accepted: 23 December 2005 / Published online: 17 October 2006

Abstract The elastic properties of $Cd_xNi_{1-x}Fe_2O_4$ (x = 0.2, 0.4, 0.6 and 0.8) spinel ferrite system synthesized by wet-chemical technique, have been studied by infra-red spectroscopy and X-ray diffraction pattern analysis before (W) and after high temperature annealing (AW). The average particle size for wet-samples was within the range 4–5 nm, which is much lower than the average particle size found for AW samples (≈85 nm). The force constants for tetrahedral and octahedral sites determined by infrared spectral analysis, lattice constant and X-ray density values by X-ray diffraction pattern analysis; have been used to calculate elastic constants. The elastic moduli for W-samples are found to be larger as compared to AW samples, which are explained on the basis of grain size reduction effect. The average crystallite size calculated from elastic data is in agreement to that determined from X-ray diffraction data analysis.

Introduction

Magnetic nano-particles of spinel ferrites are of great interest for addressing the fundamental relationship between magnetic properties and their crystal chemistry and structure. Superparamagnetism is a unique feature of magnetic nano particles and is crucially related to many modern technologies including ferrofluid technology [1], magnetocaloric refrigeration [2], contrast enhancement in magnetic resonance imaging (MRI) [3] and magnetically guided drug delivery [4].

As wet-chemically prepared ferrites normally consist of fine particles, they exhibit unusual physical properties, as compared to conventional ceramically prepared materials [5–8]. It has motivated us to synthesize the mixed spinel solid solution series $Cd_xNi_{1-x}Fe_2O_4$ (x = 0.2, 0.4, 0.6 and 0.8) by co-precipitation technique at a lower temperature (55 °C) and also to examine the effect of Cd^{2+} substitution in $NiFe_2O_4$ before (W) and after high temperature sintering (≈1100 °C) (AW) on the elastic properties.

The elastic constants are of much importance because they elucidate the nature of binding forces in solids and to understand the thermal properties of the solids. A most conventional technique for elastic constants and Debye temperature determination is the ultrasonic pulse transmission technique [9]. The sample size required for such measurements is 1 cm in length. In the study of elastic properties of recent technologically important nanoparticles, superconductors, single crystal, irradiated or specially treated materials, where sample quantity available is very small such technique may not be useful. We have developed a new method to study the elastic properties of spinel ferrites [10, 11] and garnets [12] using infrared spectroscopy, where only a few milligram of the material is sufficient for the characterization.

Infrared (IR) spectroscopy is one of the most powerful analytical techniques, which offers the possibility of chemical identification. One of the prime advantages of IR spectroscopy over the other methods

---

K. B. Modi (✉) · M. K. Rangolia · M. C. Chhantbar ·
H. H. Joshi
Department of Physics, Saurashtra University, Rajkot
360 005, India
e-mail: kunalbmodi2003@yahoo.com

of structural analysis is that it provides useful information about the structure of molecule rapidly and also without cumbersome evaluation methods. The technique is based upon the simple fact that a chemical substance shows marked selective absorption in the infrared region. After the absorption of IR radiation, the molecules of chemical substance vibrate at many rates of vibrations, giving rise to closed-packed absorption bands, called ‘‘IR Absorption spectrum’’, which may extend over a wide wavelength range. Various bands present in IR spectrums are corresponding to the characteristic functional groups and bonds present in chemical substance. Hence, an IR spectrum of a chemical substance is the fingerprint for its identification.

The aim of the present work is to look into the effect of the preparation condition on the elastic properties of $Cd_xNi_{1-x}Fe_2O_4$ ferrites system by means of X-ray diffraction and infrared spectroscopic measurements. The reasons for making EDAX characterization of the AW-samples were to test the purity and surety of the chemical composition of the wet-chemically prepared fine particle powders.

Experimental details

The spinel ferrite system $Cd_xNi_{1-x}Fe_2O_4$ with variable composition $x = 0.2$, 0.4, 0.6 and 0.8 was prepared by air oxidation of an aqueous suspension containing Ni^{2+}, Cd^{2+} and Fe^{3+} cations in stoichiometric proportions. The starting solutions were prepared by mixing 50 ml of aqueous solution of $NiSO_4{\cdot}7H_2O$, $FeSO_4{\cdot}7H_2O$ and $CdSO_4{\cdot}7H_2O$ in proper proportions. A 2 M solution of NaOH was prepared as a precipitant. In order to achieve simultaneous precipitation of all the hydroxides, the starting solution (pH value about 3.5) was added to the solution of NaOH and a suspension (pH = 10.5) containing dark green intermediate precipitates was formed. Then the suspension was heated and kept at a temperature of 55 °C, while oxygen gas was bubbled uniformly into the suspension to stir it and to promote oxidation reaction, until all the intermediate precipitates changed into the dark brownish precipitate of the spinel ferrites. The samples were filtered, washed by acetone and dried at 100 °C under vacuum for 8 h. The wet-samples (W) of Ni–Cd ferrites were sintered in air at 1100 °C for 24 h and slowly cooled to room temperature (AW samples). The preparation of ferrite powders by the oxidation method consists of oxidation by bubbling air (O_2) through an aqueous solution containing ferrous ions (Fe^{2+}) and other divalent ions (M^{2+}) after an alkaline solution (ROH) has been added, the reaction is given by:

$$Fe^{2+} + M^{2+} + ROH + O_2 \rightarrow M^{2+}_{1-x}Fe^{3+}_{2-x}O_4$$

where ROH is NaOH, KOH, NH_4OH etc. Thus, ferrite powders with high homogeneity and purity are obtained.

The X-ray powder diffractograms of all the samples of Ni–Cd ferrites were recorded using CuK_α radiation on a Philips diffractometer model (PM 9220) at 300 K. For recording IR spectra, powders were mixed with KBr in the ratio 1:100 by weight to ensure uniform dispersion in the KBr pellet. The mixed powders were then pressed in a cylindrical die to obtain clear disc. The IR spectra in the wave number range 400–4000 cm^{-1} were recorded at 300 K on Perkin–Elmer made IR spectrometer. The stoichiometry of the powdered samples was checked by energy dispersive analysis of X-rays (EDAX). The compositional values were determined within the accuracy of 1%.

Results and discussion

In the direct ceramic preparation of Ni–Cd ferrites by sintering the mixture of oxide ingredients at elevated temperature (~1100 °C) there is a possibility of volatilization of cadmium oxide [13] which in turn causes loss of stoichiometry of the final products. The preparation of the Ni–Cd ferrites is rather difficult because of the high volatility of Cd and of the large value of its ionic radius (~0.097 nm). The reaction rate can be raised by simply increasing the sintering temperature but sometimes at the expense of stoichiometry. It is difficult to find safe temperature for sintering but it is possible to synthesize the ferrite materials without fear of losing any ingredient by preparing fine particle precursors at much lower temperature (~55 °C) before subjected to sintering at elevated temperatures to obtain ceramic product.

It was essential to check the chemical composition of the each annealed-wet (AW) sample. Two representative patterns of Energy dispersive analysis of X-rays (EDAX) for $x = 0.2$ and 0.6 compositions are shown in Fig. 1. The results of EDAX given in Table 1, confirmed the expected stoichiometry. No trace of any impurity was found indicating purity of the samples. It is also clear that there is no loss of any ingredient after high temperature sintering. The EDAX results suggested that the precursors have fully undergone the chemical reaction to form the expected ferrite material. The reason for making EDAX characterization of the AW-samples was to ratify the purity and surety of the chemical composition of the wet-chemically

Fig. 1 EDAX spectra for AW-composition

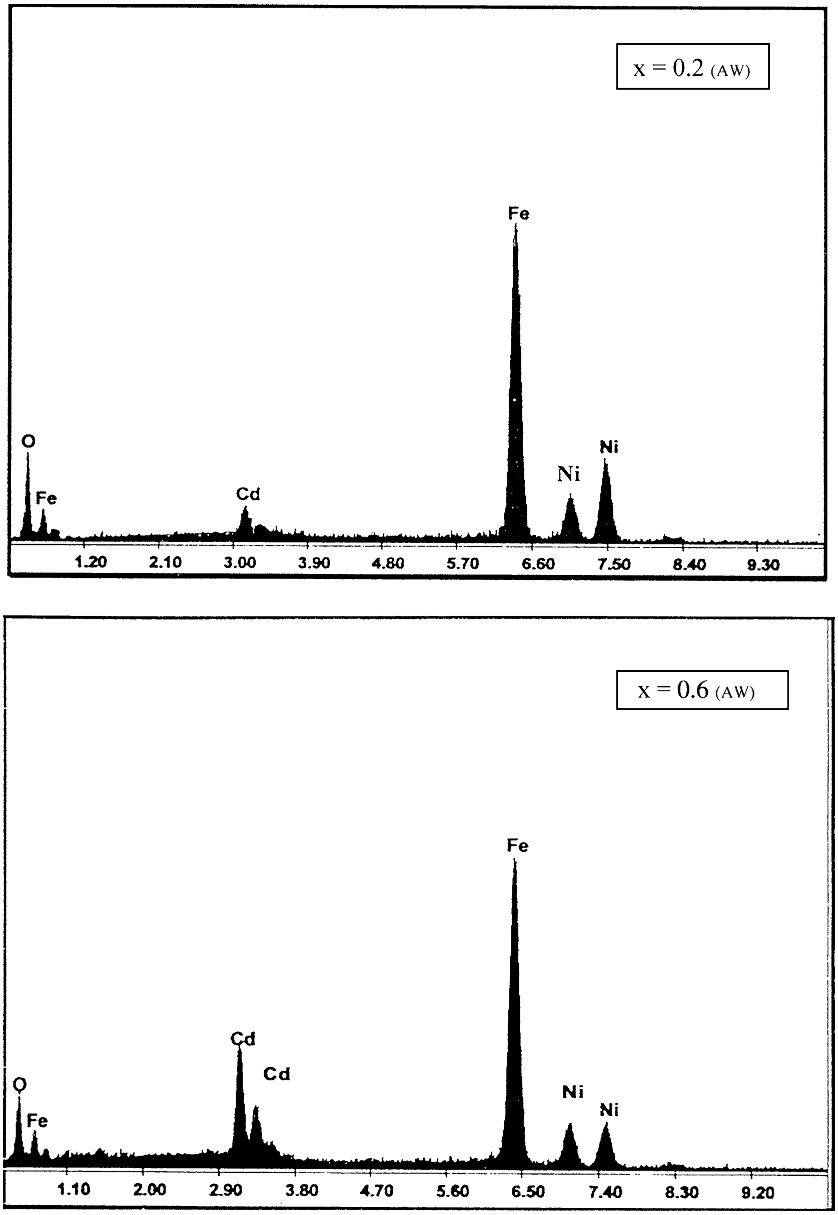

Table 1 EDAX results for AW samples of Ni–Cd–Fe–O system

Element present	$x = 0.2$		$x = 0.6$	
	Expected	EDAX	Expected	EDAX
Ni	0.80	0.78(5)	0.40	0.38(5)
Cd	0.20	0.19(4)	0.60	0.57(4)
Fe	2.00	2.02(3)	2.00	1.97(3)
O	4.00	3.98(5)	4.00	3.96(5)

prepared fine particle powders. The as-prepared samples of the wet-chemical method may contain water and hydroxyl ions which may get evaporated at high sintering temperature but if the wet-chemically prepared fine particle powders contained any access amount of Fe, Ni or Cd they would have definitely appeared after high temperature sintering in the EDAX patterns. No trace of any impurity was found, this means that the compositional stoichiometry of the Ni–Cd ferrite powders exists right from their nano-sized structure (wet-chemical products) state to ceramic sintered powders.

X-ray diffraction pattern analysis

The $Cd_xNi_{1-x}Fe_2O_4$ products of wet and annealed-wet samples were characterized by X-ray diffraction to ascertain single phase structure formation and to deduce cell-edge parameter, cation distribution and

Fig. 2 X-ray diffraction patterns for W-samples

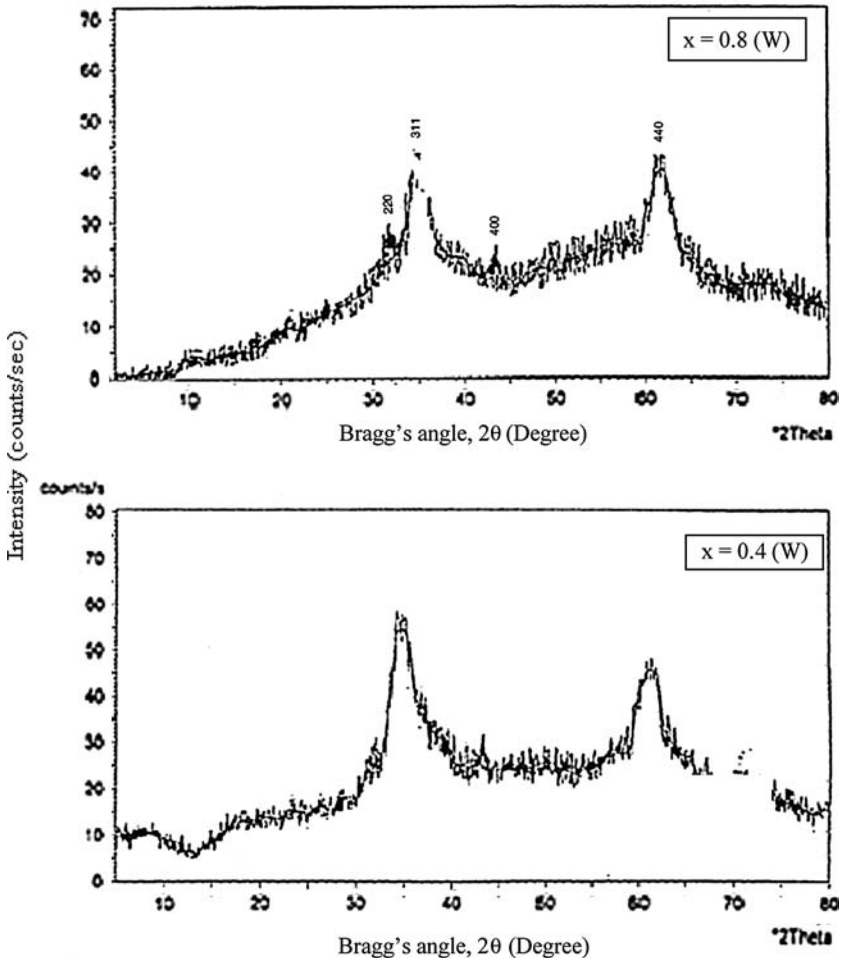

particle size. Typical X-ray diffraction patterns of wet Ni–Cd ferrite products with $x = 0.4$ and 0.8 are shown in Fig. 2. The X-ray diffractometry showed that W-samples were single phase spinels. The XRD patterns showed broad Bragg reflection lines. This is expected as the wet-samples consist of very fine particles. The Bragg reflection (311) and (440) are conspicuous while the reflection (220) and (400) are very weak. The lattice constant for W-samples found from the (440) reflection for the compositions are given in Table 2. Apart from the phase identification and lattice parameter determination, X-ray diffraction can also be used for determination of particle size from peak broadening. The average crystallite size was determined from broadening of X-ray diffraction line (440) by using the Scherrer's formula [14] with correction for instrumental broadening. The values of average particle size for the composition are shown in Table 2. The Bragg reflection peak (440) for typical W and AW-samples is shown in Fig. 3 for comparison purpose. The significant

Table 2 Lattice constant (a), average crystallite size (D), X-ray density (ρ), band position (v) and force constant (k) for wet Ni–Cd–Fe–O system

Cd-content (x)	a (nm) ±0.0002 nm	D (nm) (X-ray)	ρ (kg/m^3) × 10^3	v_1 (m^{-1}) × 10^2	v_2 (m^{-1}) × 10^2	k_t (N/m) × 10^2	k_o (N/m) × 10^2	k (N/m) × 10^2
0.2	0.8481	5.1	5.3405	666.68 601.86	463.00	2.0590	1.2975	1.6782
0.4	0.8523	4.3	5.4925	660.00 586.00	450.00	2.3210	1.2195	1.7702
0.6	0.8590	5.7	5.5900	648.16 583.34	435.18	2.5938	1.1348	1.8643
0.8	0.8623	4.8	5.7486	620.00 580.00	423.00	2.7731	1.0667	1.9199

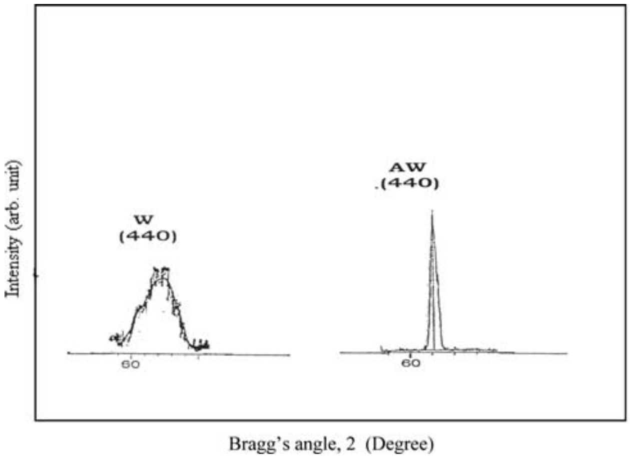

Fig. 3 Bragg's reflection (440) for W- and AW-samples

line broadening is seen due to nano-sized particle formation in wet-sample. This happens because in the nano-sized particles there are insufficient diffraction centers, which causes the line broadening. The average particle size for fine powders of wet Ni–Cd ferrites was found to be within 4–5 nm, which is much lower than the average particle size found for AW-samples (≈85 nm).

The X-ray diffraction patterns of AW-samples with x = 0.2, 0.4, 0.6 and 0.8 are shown in Fig. 4. The XRD patterns showed that all the samples were monophase spinel structure. No extra line corresponding to any other phase or unreacted ingredient was detected. The diffraction lines were found to be very sharp making detection of any impurity phase easy. It is clear that fine particle nature is lost after high temperature annealing and the ferrite materials are akin to bulk samples having coarse particles. All the diffraction patterns were indexed using computer program. It is seen that all the diffraction patterns could be indexed for face centered cubic (fcc) structure. The lattice constant for each composition was found using Nelson–Riley method [14] (Table 3).

The concentration dependence of lattice constant "*a*" with an accuracy of ±0.0002 nm determined from X-ray data is presented in Tables 2, 3 for W and AW system, respectively. The lattice constant gradually increases with increasing x, obeying Vegard's law [15], is due to replacement of smaller Ni^{2+} (0.069 nm) ions by larger Cd^{2+} (0.097 nm) in the $Cd_xNi_{1-x}Fe_2O_4$ system. The X-ray density for each composition was calculated using the relation [14]: $\rho = ZM/Na^3$, where Z is the number of molecules per unit cell (Z=8) of the spinel lattice, M is the molecular weight of the ferrite sample, N is the Avogadro's number and "*a*" is the lattice constant. The variation of X-ray density (ρ) with concentration (x) is shown in Tables 2, 3 for W and AW samples, respectively. In the present case, X-ray density increases in spite of the increase in lattice constant with increasing x. This is due to the fact that, increase in mass (M) overtakes the increase in volume of the unit cell (a^3) in the system.

The cation distributions for the spinel oxide materials are determined by comparing the observed calculated X-ray diffraction intensity values for the planes sensitive to the variation in distribution for the present system is:

$$(Cd_x^{2+}Fe_{1-x}^{3+})^A[Ni_{1-x}^{2+}Fe_{1+x}]^B O_4^{-2} \tag{1}$$

Infra red spectroscopy

Far-infrared absorption spectroscopy has been used to study the occurrence of various absorption bands in the spectra and analyzed on the basis of different cations present on tetrahedral (A-) and octahedral (B-) sites of spinel lattice [10, 11, 16–18]. It is also used to determine the local symmetry in crystalline solids, non-crystalline solids, ordering phenomenon in spinels, presence/absence of Fe^{2+} ions and also to determine force constants [10, 11, 16–18] and elastic moduli [10, 11, 16] of ferrite systems.

The room temperature (300 K) infra-red spectra for $Cd_xNi_{1-x}Fe_2O_4$ system for wet and annealed-wet samples are shown in Figs. 5, 6, respectively. It can be seen that the IR spectrum of Cadmium substituted nickel ferrites are found to exhibit two bands in the range 400–700 cm^{-1}. No absorption bands were observed above 700 cm^{-1}. The high frequency band v_1 is in the range 545–650 cm^{-1} and the lower frequency band in the range 400–425 cm^{-1}. These bands are common features of all the ferrites [16]. According to Waldron's classification [16], the vibrations of the unit cell of cubic spinel can be constructed in the A- and B-sites. So, the absorption band v_1 is caused by the stretching vibration of the tetrahedral metal–oxygen bond, and the absorption band v_2 is caused by the metal–oxygen vibration in octahedral sites. The IR absorption bands for wet-samples (Fig. 5) at 3400 cm^{-1} and 1600 cm^{-1} are assigned to adsorbed water hydroxyl ions and 1100 cm^{-1} to sulphate ions. It is seen that for AW samples the bands corresponding to water and sulphate ions are disappeared (Fig. 6) which is due to the effect of high temperature (1100 °C) sintering process for AW samples. The band positions for all the W- and AW-compositions are given in Tables 2, 3, respectively. The change in the band position is expected because of

Fig. 4 (**a**) X-ray diffraction patterns for AW-samples. (**b**) X-ray diffraction patterns for AW-samples

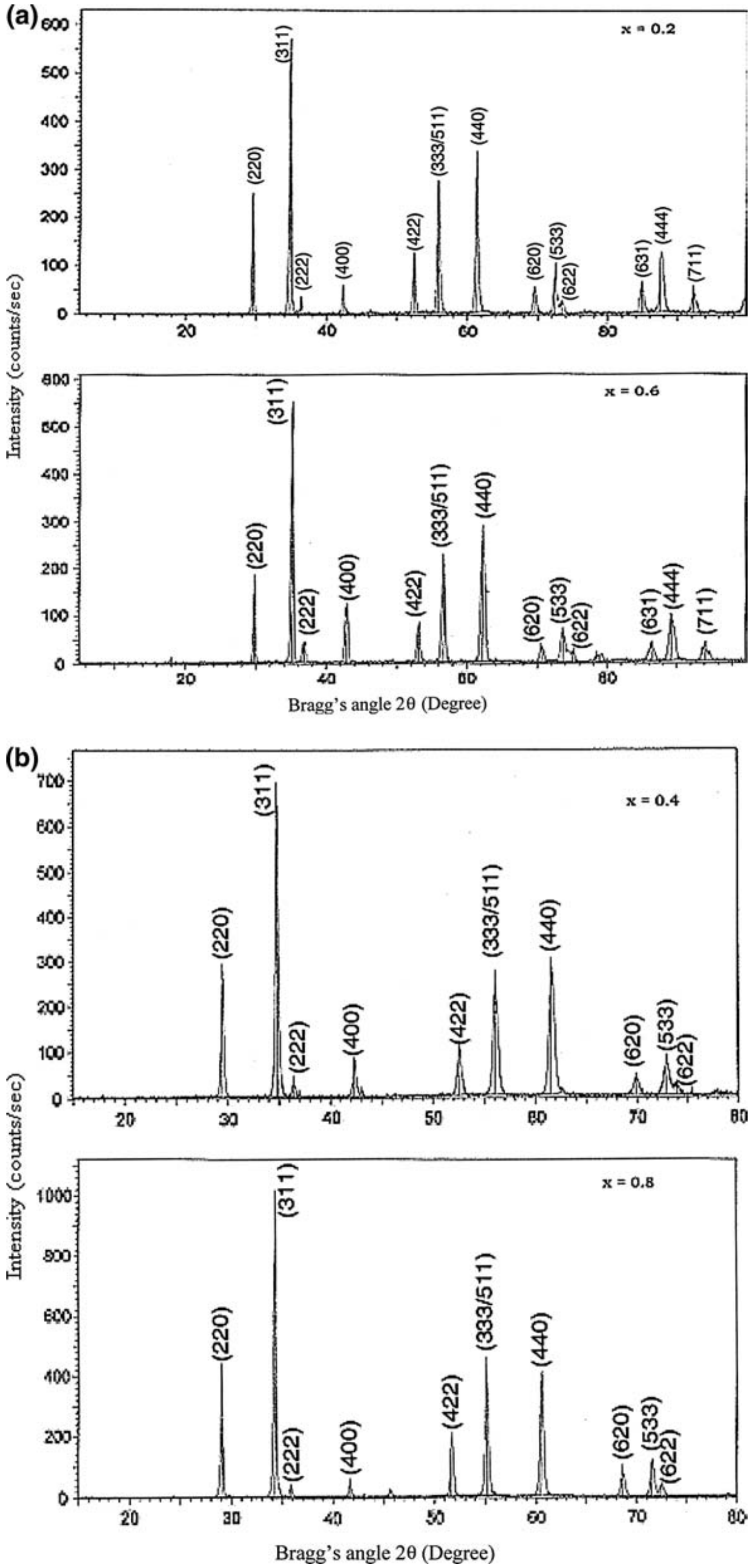

the difference in the Fe^{3+}–O^{2-} distances for the octahedral and tetrahedral complexes. It was found that Fe–O distance of A-site (0.189 nm) is smaller than that of the B-site (0.199 nm) [19]. This can be interpreted by the more covalent bonding of Fe^{3+} ions at the A-sites than B-sites. It is important to note that

Table 3 Lattice constant (a), X-ray density (ρ), band position (ν) and force constant (k) for AW Ni–Cd–Fe–O system

Cd-Content (x)	a (nm) ±0.0002 nm	ρ (kg/m^3) × 10^3	ν_1 (m^{-1}) × 10^2	ν_2 (m^{-1}) × 10^2	k_t (N/m) × 10^2	k_o (N/m) × 10^2	k (N/m) × 10^2
0.0	0.8385[26]	5.28	593	404[27]	1.496	0.993	1.245
0.2	0.8508	5.30	584	408	1.745	1.007	1.376
0.4	0.8552	5.44	577	408	1.991	1.003	1.500
0.6	0.8629	5.51	566	409	2.192	1.002	1.597
0.8	0.8659	5.68	554	410	2.364	1.002	1.683
1.0	0.8672[26]	5.87	548	412[28]	2.572	1.007	1.789

nature of bands remain same for wet- and AW samples, of course for wet-samples bands appear towards higher frequency side as compared to AW-samples as well as for wet-samples splitting of bands is also well resolved (Fig. 5).

The center frequency of the bands ν_1 and ν_2 shift slightly towards lower frequency side for W and AW series of compositions. It is known that increase in site radius reduces the fundamental frequency and therefore, the center frequency should shift towards lower frequency side. The increase in site radius may be expected due to replacement of smaller Ni^{2+} ions (0.069 nm) by larger Cd^{+2} (0.097 nm) in the system. Furthermore, shifting of ν_1 band towards lower frequency side is more pronounced as compared to ν_2 band. This is due to the fact that substituted Cd^{2+} ions preferentially occupy A-site only and the difference in ionic radius of A-site cations Fe^{3+} (0.064 nm) and Cd^{2+} (0.097 nm) is much larger as compared to B-site cations Fe^{3+} (0.064 nm) and Ni^{2+} (0.069 nm) in the system (Eq. 1).

It is important to note that on increasing Cd^{2+}-content (x) in the system, bands become more and

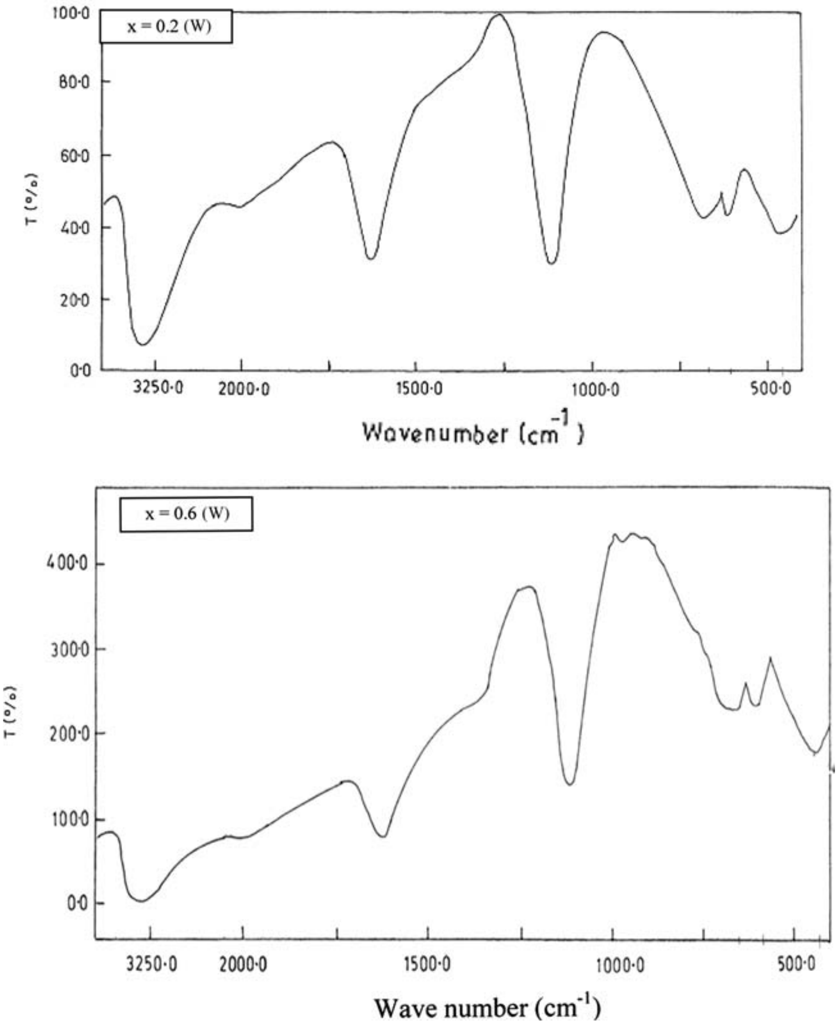

Fig. 5 Infra-red spectra of W-samples

Fig. 6 (**a**) Infra-red spectra of AW-samples. (**b**) Infra-red spectra of AW-samples

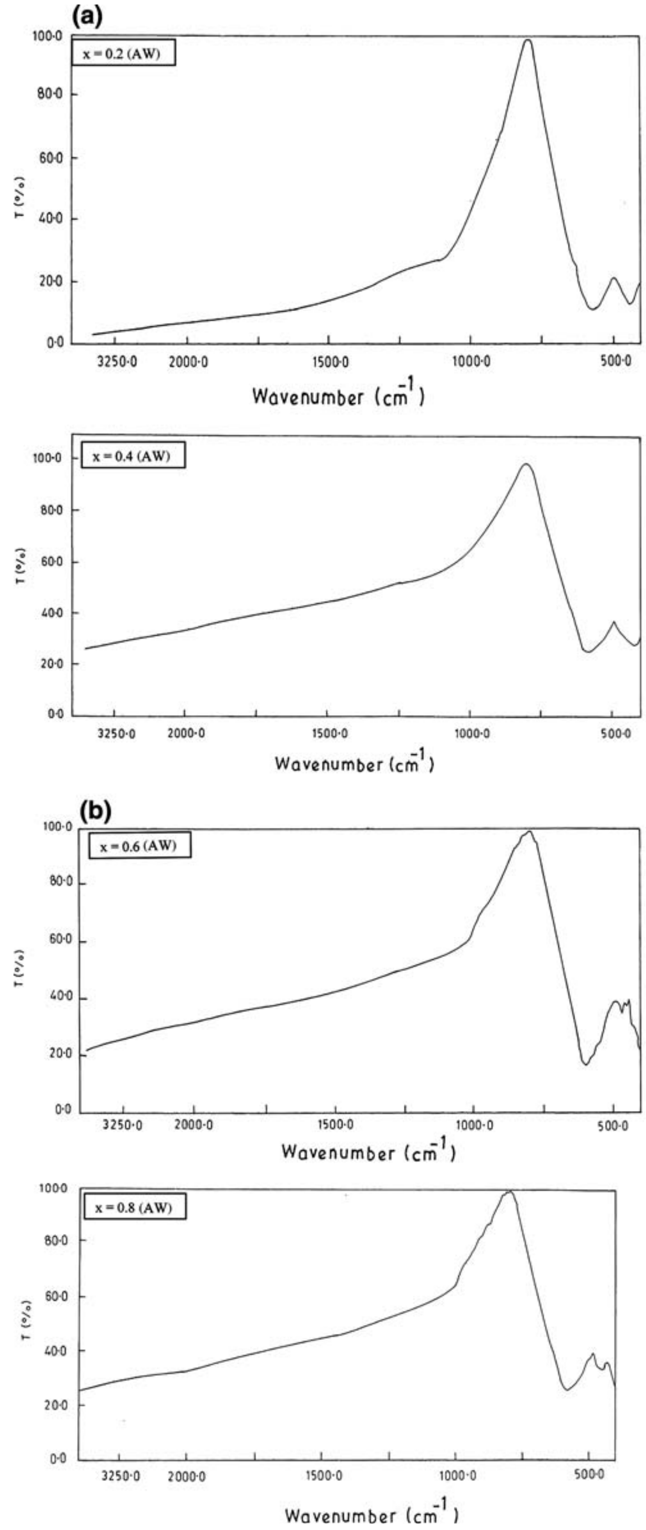

more broader (Figs. 5, 6). The broadening of bands has been reported earlier by many workers [18, 20–22]. Bellad et al. [22] have observed an increase in broadening for higher content of cadmium in the case of Li–Cd ferrites. They have reported that such broadening is commonly observed in normal spinel ferrites and have attributed it to the statistical distribution of Fe^{3+} ions as A- and B-sites. In the present case, system transfer from inverse $NiFe_2O_4$ ($x = 0.0$) to normal ($CdFe_2O_4$) ($x = 1.0$) spinel structure as confirmed by cation distribution formula (Eq. 1), results in broadening of bands.

Elastic properties

The force constant is a second derivative of potential energy with respect to the site radius, the other independent parameters being kept constant. The force constants, for tetrahedral site (k_t) and octahedral site (k_o), were calculated employing the method suggested by Waldron [16]. According to Waldron, the force constants, k_t and k_o, for respective sites are given by

$$k_{\mathrm{t}} = 7.62 \times M_1 \times v_1^2 \times 10^{-7}\,\mathrm{N/m}$$
$$k_{\mathrm{O}} = 10.62 \times M_2/2 \times v_2^2 \times 10^{-7}\,\mathrm{N/m}$$

where M_1 and M_2 are the molecular weights of cations on A- and B-sites, respectively, calculated from cation distribution formula (Eq. 1). The variation of force constants with Cd-content (x) for W-samples and AW-samples are shown in Tables 2, 3, respectively.

A most conventional technique for elastic constants and Debye temperature determination is the ultrasonic pulse transmission technique [23, 24]. We have developed a new method to study the elastic properties of spinel ferrite and garnet systems by infrared spectroscopy [10–12] and it is expected to generalize for other materials also. This technique is extremely useful for the nano-sized powders synthesized by the wet-chemical route to reveal the unwanted surface-adsorbed ions through the infrared absorption bands.

The bulk modulus (B) of solids in terms of stiffness constants is defined as $B = 1/3[C_{11} + 2C_{12}]$, but according to Waldron et al. [16] for isotropic materials with cubic symmetry like spinel ferrites and garnets, $C_{11} \approx C_{12}$, therefore, B is simply given by C_{11}. Further, force constant (k) is a product of lattice constant (a) and stiffness constant (C_{11}) [9]. The values of lattice constant and average force constant ($k = (k_t + k_o)/2$) for wet- and AW-samples have been used for calculating B and are given in Tables 4, 5, respectively. We have determined the value of longitudinal elastic wave velocity (V_l) using the formula suggested by Waldron [16] $V_l = (C_{11}/\rho)^{1/2}$ and the transverse elastic wave velocity (V_s) by general approximation $V_l = 3^{1/2} \cdot V_s$ [24–25]. The values of V_l and V_s are further used to calculate the elastic moduli and Debye temperature of the ferrite specimens using the following formulae [25]:

$$\text{Rigidity modulus } (G) = \rho \mathrm{V}_\mathrm{s}^2$$
$$\text{Poisson's ratio } (\sigma) = 3B - 2G/6B + 2G$$
$$\text{Young's modulus } (E) = (1 + \sigma)2G$$
$$\text{Mean elastic wave velocity } (\mathrm{V}_\mathrm{m}) : [3(\mathrm{V}_\mathrm{s}^3 \cdot \mathrm{V}_\mathrm{l}^3/\mathrm{V}_\mathrm{s}^3 + 2\mathrm{V}_\mathrm{l}^3)]^{1/3}$$
$$\text{Debye temperature } (\theta) : \; h/k_\mathrm{B}[3N_\mathrm{A}/4\pi V_\mathrm{A}]^{1/3} \cdot V_\mathrm{m}$$

where, V_A is mean atomic volume given by $(M/\rho)/q$, M the molecular weight, and q is the number of atoms (i.e. 7) in the formula unit, N_A, is Avogadro's number. It can be seen that for wet- and AW-samples, E, B and G increase with increasing Cd^{2+} content (x), indicate that the corresponding deformation of the solid is difficult and that the solid has a strong tendency to "spring" (analogous to planes within a solid held to

Table 4 Elastic wave velocity (V), elastic constants, Poisson's ratio (σ) and Debye temperature (θ) for wet Ni–Cd–Fe–O system

Cd-content (x)	V_l (m/s)	V_s (m/s)	V_m (m/s)	E (GPa)	B (GPa)	G (GPa)	σ	θ (K)	D (nm) (elastic data)
0.2	6087.1	3514.4	3901.7	178.0	197.8	65.9	0.35	524.2	4.66
0.4	6139.0	3544.4	3934.9	186.3	207.7	69.0	0.35	526.1	5.49
0.6	6230.9	3597.4	3993.8	195.3	217.0	72.3	0.35	529.8	5.77
0.8	6223.4	3593.1	3989.1	200.4	222.0	74.2	0.35	527.2	19.71

Table 5 Elastic wave velocity (V), elastic constants, Poisson's ratio (σ) and Debye temperature (θ) for AW Ni–Cd–Fe–O system

Content (x)	V_l	V_s	V_m	E	B	G	σ	θ (K)
0.0	5302.5	3061.3	3398.6	133.6	148.4	49.5	0.35	461.8
0.2	5524.4	3189.5	3540.9	145.6	161.8	53.9	0.35	474.6
0.4	5671.8	3274.6	3635.5	157.5	175.0	58.3	0.35	484.5
0.6	5795.2	3345.9	3714.6	166.5	185.1	61.7	0.35	490.5
0.8	5760.3	3325.7	3692.2	209.0	188.5	77.4	0.35	485.9
1.0	5929.0	3423.1	3800.4	228.9	206.4	84.8	0.35	499.4

gather by atomic bond) back to its equilibrium position. The Poisson's ratio, however, remains constant for different compositions. The value of σ is found to be 0.35 for both the set of samples (W- and AW), this value lies in the range from –1 to 0.5, which is in conformity with the theory of isotropic elasticity. On the other hand, for AW-samples, the observed increase in θ suggested that lattice vibrations are hindered due to cadmium substitution. This may be due to the fact that strength of interatomic bonding increases with the replacement of Ni^{2+} by Cd^{2+} in $Cd_xNi_{1-x}Fe_2O_4$ system as supported by our results on variation of elastic moduli with Cd-content. However, observed change in θ for wet samples is very small as compared to AW-compositions.

The elastic moduli values for fine grained ferrites found to be larger as compared to coarse grained AW-compositions (Tables 4 and 5). The size of the grains, average grain diameter of a polycrystalline powder influences the mechanical properties. Adjacent grains normally have different crystallographic orientation and of course, a common grain boundary. The grain boundary acts as a barrier to strain motion. A fine-grained material is harder and stronger than one that is coarse grained, since the former has a greater total grain boundary area to impede dislocation motion. It should also be mentioned that grain size reduction improves not only strength but also the toughness of materials. Grain size may be regulated by appropriate preparative parameters.

It is important as well as interesting to note that elastic moduli and Debye characteristic temperature determined through ultrasonic pulse transmission technique for Ni–Cd ferrite system synthesized by conventional double sintering ceramic technique, show reduction in magnitude with increasing cadmium concentration in the $Cd_xNi_{1-x}Fe_2O_4$ system [24]. In the present case, they are found to increase with increase in Cd-content (x), suggest that it is possible to change the magnitude and trend of compositional variation of elastic constants by controlling preparative parameters. Based on this it is clear that, wet-chemical technique proved to be better as compared to ceramic technique as far as elastic properties are concern.

It is now clear that particle size and elastic moduli have inverse relationship. It is possible to estimate particle size for wet-samples using the values of elastic constants of W- and AW-samples determined through IR-spectroscopy and particle size of AW-sample, using the formula:

$$\frac{P_{AW}}{P_W} = \left[1 - \frac{K_{AW}}{K_W}\right] \cdot 100$$

Where P_W and P_{AW} are particle size of wet- and AW samples, K_W and K_{AW} are elastic moduli (E, G or B) of the W- and AW compositions. This formulation is analogous to the porosity determination formula from corresponding bulk and X-ray density values [14]. The value of particle size thus calculated (Table 4) is in good agreement to those determined from X-ray diffraction pattern analysis, validates the method used. Further more, this method is quite simple as compared to conventional method of particle size determination by scanning electron microscopy (SEM) and permeability measurements.

Conclusions

In conclusion, (i) Nano-sized crystallites of Ni–Cd mixed ferrite materials can be synthesized by co-precipitation (wet-chemical) technique and single phase stoichiometric coarse micron-sized particles can be obtained by high temperature sintering of these fine particle precursors without loss of cadmium. (ii) Elastic moduli and Debye temperature can be determined through IR spectral analysis and observed increase of elastic constants with cadmium-substitution suggests strengthening of interatomic bonding. (iii) The larger value of elastic constants for fine-particle compositions as compared to coarse grained annealed wet ferrites is due to large elastic energy and grain size reduction effect. (iv) Particle size estimated from elastic data is in good agreement to those calculated from X-ray diffraction data analysis.

Acknowledgement One of the authors (KBM) is thankful to All India Council of Technical Education (AICTE), New Delhi, for providing financial assistance in the form of career award for young teachers (2004). This work is financially supported by Nuclear Science Center, New Delhi under UFUP project scheme of Prof. H.H. Joshi.

References

1. Raj K, Moskowitz R, Casciari R (1995) J Magn Magn Mater 149:174
2. McMichael RD, Shull RD, Swartzenruber LJ, Bennett LH (1992) J Magn Magn Mater 111:29
3. Mitchel DG (1997) J Magn Reson Imaging 7:1
4. Hafeli U, Schutt W,Teller J, Zborowski M (Eds) (1997) Scientific and clinical applications of magnetic carriers. Plenum, New York
5. Borriesci N, Garbassi F, Pizzini JS (1978) J Magn Magn Mater 7:52
6. Liu C, Rondinone J, Zhang Z (2000) Pure Appl Chem 72:37
7. Upadhyay C (2003) Ph.D. Thesis, IIT-Kanpur, India
8. Jadhav KM, Kawade VB, Modi KB, Bichile GK, Kulkarni RG (2000) Physica B 291:379

9. Kakani SL, Hemrajani CA (1997) Text book of solid state physics, 3rd ed. Sultan Chand & Sons, New Delhi, pp 150 and 190
10. Modi KB (2004) J Mater Sci 39:2887
11. Modi KB, Trivedi UN, Pandya MP, Bhatu SS, Chhantbar MC, Joshi HH (2004). In: Shirsat MD (ed) Microwaves and optoelectronics. Anamaya Publishers, New Delhi, p 223
12. Modi KB, Sharma PU, Chhantbar MC, Joshi HH (2005) J Mater Sci 40(5):1247
13. C.R.C. Hand book of physics and chemistry
14. Cullity BD (1978) Elements of X-ray diffraction, 2nd ed. Addison-Wesley Pub. Co, Reading, MA
15. Winfrey CG, Eckart DW, Tauber A (1960) J Am Chem Soc 82:2695
16. Waldron RD (1955) Phys Rev 99:1727
17. Ravinder D (1999) Mater Lett 40: 205 references there in
18. Ladgaonkar BP, Kolekar CB, Vaingankar AS (2002) Bull Mater Sci 25:351
19. Evans BJ, Hafner S (1968) J Phys Chem Solids 29:1573
20. Trivedi UN, Modi KB, Jani KH, Joshi HH (2000) J Mater Sci lett 19:1271
21. Josyula OS, Sobhandri J (1981) Phys Status Solid A65:479
22. Bellad SS, Pujar RB, Chougale BK (1998) Ind J Pure Appl Phys 36:598
23. Laurance Meixner D, Cutler RA (2002) Solid State Ionic 146:273 159 (2003) 9
24. Ravinder D, Manga T (1999) Mater Lett 41:254 references there in
25. Raj B, Rajendram V, Palanichamy P (2004) Science and technology of ultrasonics, 250. Narosa Pub. House, New Delhi
26. Swamy PM, Nagrajan T, Naryanswamy A (1981) Phys Stat Solid (a) 64:747
27. Grimes NW, Collet AJ (1971) Nature (Phys Sci) 230:158
28. Predhomme J Tarte P (1971) Spect Chim Acta 279:1817